VII International Conference on Computational Methods in Marine Engineering
MARINE 2017
M. Visonneau, P. Queutey and D. Le Touzé (Eds)

# SIMULATION OF FLOATING BODIES USING A COMBINED IMMERSED BOUNDARY WITH THE LEVEL SET METHOD IN REEF3D

**HANS BIHS*, ARUN KAMATH*, JIAYI ZHENG LU* AND ØIVIND A. ARNTSEN***

*Department of Civil and Environmental Engineering
NTNU Trondheim
Høgskolereingen 7A, 7491 Trondheim, Norway
e-mail: hans.bihs@ntnu.no, web page: http://www.reef3d.com/

**Key words:** CFD, REEF3D, 6DOF, floating body, free surface flow, level set method

**Abstract.** The 6DOF algorithm implemented in the open-source computational fluid dynamics (CFD) model REEF3D is used to simulate a horizontal cylinder in heave motion around the free surface and the motion of a freely floating rectangular barge in waves. The numerical model uses a staggered Cartesian grid. The free surface is obtained with the level set method. The floating body is described with a primitive triangular surface mesh neglecting connectivity. A ray-tracing algorithm is used to determine the intersection of this surface mesh with the underlying Cartesian grid. In this way, the model avoids re-meshing the domain while calculating the motion of the floating object. The moving fluid-solid boundary is treated with the immersed boundary ghost cell method. In order to validate the model, two test cases are presented. First, the damping of the heave motion after providing an initial excitation by raising the center of gravity of the cylinder slightly above the free surface is calculated and the numerical results are compared to experimental data. Then, the motion of a freely floating rectangular barge is simulated under different wave conditions. The barge is free to move in surge, roll and heave motions. The numerical results are compared to the experimental results to validate the algorithm. The results show that the numerical model REEF3D represents the motion of floating objects well, with good agreement with the experimental results.

## 1 INTRODUCTION

A large number of engineering problems in various fields involve fluid-structure interaction. In the field of marine and coastal engineering, the fluid structure problem is further challenging due to the presence of the free surface. The free surface interaction plays an important role in the hydrodynamics of a floating structure. With several important economic activities in the domain of marine engineering, it is essential to develop a better understanding of the interaction of the floating bodies on water such as ships, floating piers, floating breakwaters or floating ice floes. Such investigations have been traditionally carried out using physical experiments. With

the advances in computational modelling, deep insights into the fluid-floating body hydrodynamics can be obtained through numerical modelling. Here, solving the Navier-Stokes equations can calculate complex physical processes involved in the interaction problem such as the viscous effects from turbulence, complex free surface phenomena due to the impact of an object and non-linear effects on the body due to non-linear wave events.
An earlier approach to fluid-structure interaction Navier-Stokes solvers has been to use Arbitrary Lagrangian-Eulerian (ALE) methods [17], [21]. When the structure is moving, the underlying mesh is re-adjusted in order to track the movement of the solid. For complex flow situations as often encountered in the field of marine engineering, this can limit the applicatbility of the algorithm. More flexibility is achieved, when two individual grids are used, one for the underlying fluid flow and another for the moving solid. The overset mesh implementation (e.g. [5]) avoids re-meshing at the cost of continuously re-mapping the overset region. Yang et al. [22] presented a two-phase flow solver with a sharp interface immersed boundary method for embedding the moving solids in the fluid flow. This way, the grid remains fixed and avoids re-meshing as well as the operations needed for the overset mesh approach.
In the current study the 6DOF algorithm in REEF3D is present. REEF3D is an open-source CFD code, developed at the Department of Civil and Environmental Engineering at Norwegian University of Science and Technology (NTNU), Norway. The software has been successfully used for several marine applications, such as wave forces and free surface analysis around horizontal cylinders in tandem[15], waves forces and wave elevation around vertical cylinders [13] or breaking wave forces [4]. At first, the model is validated with a free heaving of a circular disk case. Then, the free floating of a rectangular box is investigated for wave conditions.

## 2 NUMERICAL MODEL

The numerical simulations in the present paper are performed with the open-source CFD code REEF3D [3]. For the hydrodynamics of the flow, the continuity equation and the incompressible Reynolds-Averaged Navier-Stokes equations are solved:

$$\frac{\partial u_i}{\partial x_i} = 0 \tag{1}$$

$$\frac{\partial u_i}{\partial t} + u_j \frac{\partial u_i}{\partial x_j} = -\frac{1}{\rho}\frac{\partial p}{\partial x_i} + \frac{\partial}{\partial x_j}\left[(\nu + \nu_t)\left(\frac{\partial u_i}{\partial x_j} + \frac{\partial u_j}{\partial x_i}\right)\right] + g_i \tag{2}$$

where $u$ is the velocity $t$, $\rho$ is the fluid density, $p$ is the pressure, $\nu$ is the kinematic viscosity, $\nu_t$ is the eddy viscosity and $g$ the acceleration due to gravity. For turbulence, the two-equation $k-\omega$ model is selected. Additional limiters for the eddy-viscosity [8] and turbulence at the free surface [14] are included to avoid turbulence over-production typical for oscillatory two-phase flow, see [3] for details. The convective terms of the Navier-Stokes equation are treated with the fifth-order accurate conservative WENO (weighted essentially non-oscillatory) scheme in a finite difference framework [12]. The second-order TVD Runge-Kutta scheme is used for the temporal discretization [19], while the time step is selected adaptively based on the CFL number [7]. The transport equations of the turbulence model are solved implicitly, in order to avoid the time step restrictions arising from the large source terms for turbulence production and dissipation. The pressure is treated with the projection method [6] and the resulting Poisson equation is solved

using HYRPE's geometric multigrid PFMG [1] preconditioned BiCGStab solver [9].
The free water surface aspect of the flow is considered through a two-phase flow approach. For the interface capturing, the level set method is used [16]. The free surface is then the zero-contour of the signed distance function $\phi$ with the following properties:

$$\phi(\vec{x},t)\begin{cases} > 0 \; if \; \vec{x} \in phase \; 1 \\ = 0 \; if \; \vec{x} \in \Gamma \\ < 0 \; if \; \vec{x} \in phase \; 2 \end{cases} \tag{3}$$

The level set function is propagated with a simple convection equation, where the Hamilton-Jacob version of the WENO scheme [11] is used for spatial discretization:

$$\frac{\partial \phi}{\partial t} + u_j \frac{\partial \phi}{\partial x_j} = 0 \tag{4}$$

Under the flow propagation, the level set function tends to loose its signed distance property, making re-distancing necessary. The current approach uses the PDE based level set reinitialization [20]:

$$\frac{\partial \phi}{\partial t} + S\left(\phi\right)\left(\left|\frac{\partial \phi}{\partial x_j}\right| - 1\right) = 0 \tag{5}$$

Both equations Eqs. 4 and 5 use the third-order TVD Runge-Kutta scheme [19] for advancing in time. For the simulation of the free floating box, waves are generated using the relaxation method [3].

## 3 6DOF ALGORITHM

An overview of the fluid-structure interaction algorithm for the floating body is presented [2]. A triangular surface mesh without connectivity is created to define the geometry of the body. A ray-tracing algorithm, calculating the shortest distance to the closest triangle for the grid point, is used to determine the intersections of the surface mesh with the underlying Cartesian grid. The level set method is used to define the solid boundary of the floating object. The standard reinitialization algorithm is used to obtain signed distance properties for the level set function in the vicinity of the solid body. The forces on the surface $\Omega$ are determined for each direction $i$ separately with the pressure $p$ and the viscous stress tensor $\tau$:

$$F_{i,e} = \int_{\Omega} (-\mathbf{n}_i p + \mathbf{n_i} \cdot \tau) d\Omega \tag{6}$$

The moments around the center of gravity can be calculated with the following equation:

$$L_{i,cg} = \int_{\Omega} \mathbf{r}_{cg} \; \times (\mathbf{n_i} p + \mathbf{n_i} \tau) d\Omega \tag{7}$$

As the outer geometry of the floating body is represented through a level set function, the discrete surface area can be determined with a Dirac delta function:

$$d\Omega = \int \delta(\phi) |\nabla \phi| dx \tag{8}$$

The dynamic rigid body equations can be solved based on the forces $X, Y, Z$, the moments $K, M, N$ and the moments of inertia $I_x, I_y, I_z$:

$$\begin{aligned} F_i &= \mathbf{J_1^{-1}} F_{i,e} = [X, Y, Z] \\ L_i &= \mathbf{J_1^{-1}} L_{i,e} = [K, M, N] \end{aligned} \tag{9}$$

with the equations of motions for the six degrees of freedom:

$$\begin{aligned} [m(\dot{u} - \nu r + \omega q)] &= X \\ [m(\dot{\nu} - \omega r + \nu q)] &= Y \\ [m(\dot{\omega} - \nu r + \omega q)] &= Z \\ [m(\dot{\omega} - \nu r + \omega q)] &= Z \\ [I_x(\dot{p} + (I_z - I_y)qr] &= K \\ [I_y(\dot{q} + (I_x - I_z)rp] &= M \\ [I_z(\dot{r} + (I_y - I_x)pq] &= N \end{aligned} \tag{10}$$

where $u, v, w$ are the linear velocities and $p, q, r$ the angular velocities. Then $\dot{u}, \dot{v}, \dot{w}, \dot{p}, \dot{q}$ and $\dot{r}$ can be calculated in an explicit manner.
The generic linear or angular velocities $\dot{\varphi}$ and the generic position or orientation vector $\varphi$ of the floating body can be calculated with a second-order Adams-Bashforth scheme for the new time-step:

$$\begin{aligned} \dot{\varphi}^{n+1} &= \dot{\varphi}^t + \frac{\Delta t}{2}\left(3\ddot{\varphi}^{n+1} - \ddot{\varphi}^n\right) \\ \varphi^{n+1} &= \varphi n + \frac{\Delta t}{2}\left(3\dot{\varphi}^{n+1} - \dot{\varphi}^n\right) \end{aligned} \tag{11}$$

The dynamic rigid body equations are solved in the floating body reference frame, while the fluid forces and moments are calculated in the earth-fixed reference frame. As a result, coordinated transformations in both directions are necessary [5][2].

## 4 RESULTS

### 4.1 Heaving of a Circular Cylinder

For validation purposes, a 2D free heaving body is simulated. The movement of the body is limited to the vertical degree of freedom and it is allowed to oscillate freely. Experimental studies has been performed by Ito [10] with a circular cylinder and the data will be used for comparison with the numerical model. The spatial domain of the numerical wave tank (NWT) is 10m long and 1.8m high. The water depth is $d$=1.22m and the water is initially still. The density of the water is $\rho$=1000kg/m$^3$.

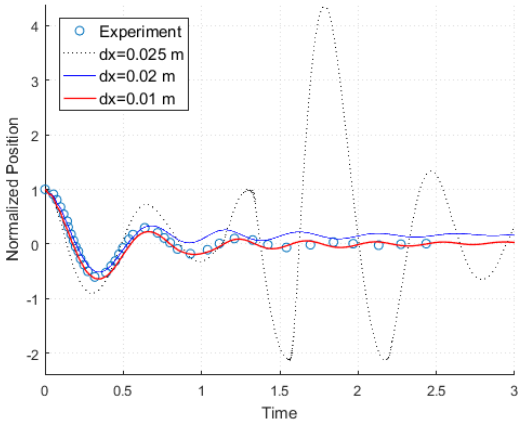


Figure 1: Comparison of three grids with experiment data

The configuration of the body position follows Ito's [10] set up where the object is located in the centre of the tank. The body is a horizontal circular cylinder with a radius $r$=0.0762m and half of water density, $\rho$=500kg/m$^3$. The cylinder is partially submerged with its centroid at $h_1$=0.02454m above the free surface. The cylinder is released from this initial position in a free fall and enters the water. A uniform grid in the domain is used for the simulations, there are three different mesh sizes used: 0.025m, 0.02m and 0.01m with a grid size of 400x72, 500x90 and 2000x180 in the horizontal and vertical directions, respectively.

Results presented in Fig. 1 have a normalized Z-axis subtracting the water depth and dividing by the initial displacement $h_i$ while the X-axis represents time.

$$Normalization = \frac{Z - d}{h_i} \tag{12}$$

In Fig. 1, the mesh size of 0.025m approximates the experiment in the first oscillation but diverges from there, having a high oscillation after 1.5s. The 0.02m grid size is closer to the experiment data, however the oscillations start to differ after 1s. The mesh size of 0.01m matches the experimental data, representing the behaviour of the cylinder correctly. After 1.5s the position start to differ slightly, due to the effect of the reflected waves generated from the left and right side walls. The mesh size of 0.01m will be used for additional analysis.
Snapshots in 0.5s time steps until $t$=4.0s are shown in Fig. 2 . The cylinder breaks the water surface, creating a series of waves to the sides that dissipates over time and length of the tank. It can be seen that the highest velocity occurs at $t$=0.5s when the cylinder enter and breaks the still water surface. After that, waves are created at both sides, disappearing at $t$=3.0s. The release height is not enough to produce a total immersion of the cylinder which would create a water jet and separation of the free water surface. The water surface matches well with numerical simulations carried out by Yang [22]. The vorticity is shown in Fig. 3 with an horizontal line representing the water level and the boundary between air and water.

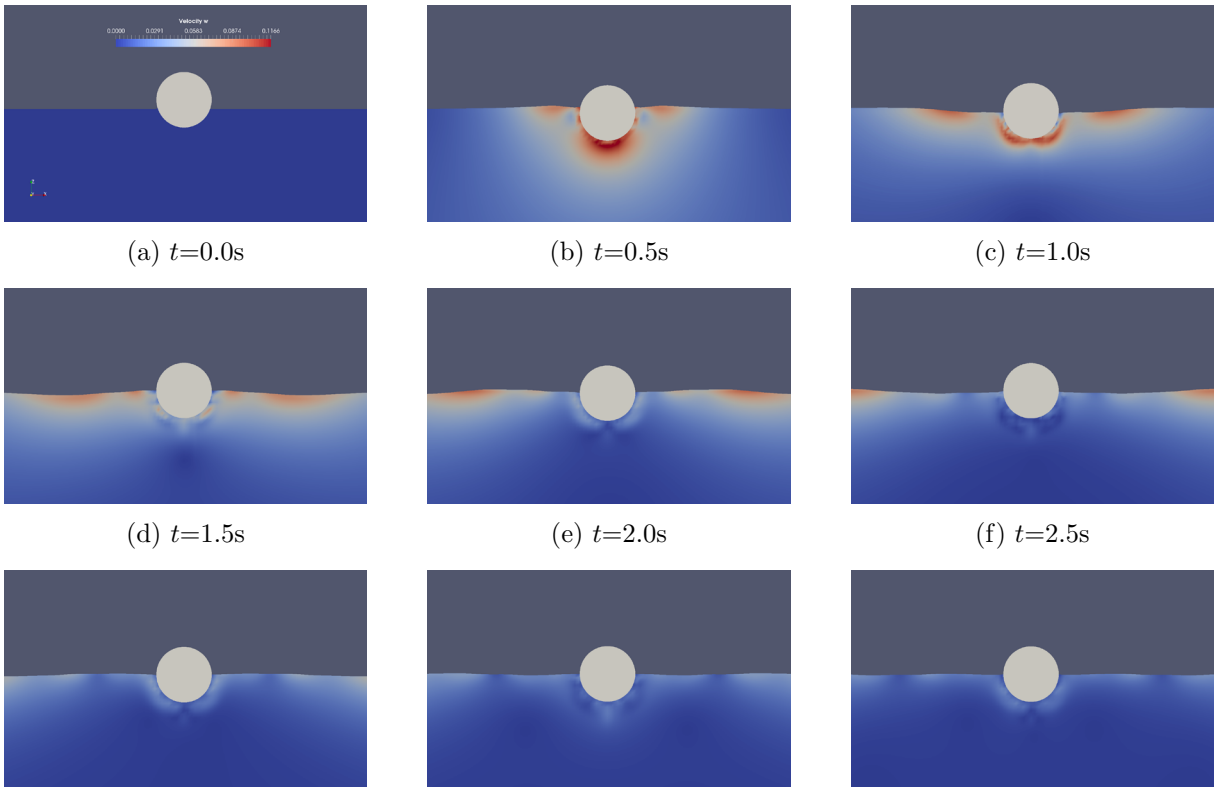

(a) $t$=0.0s (b) $t$=0.5s (c) $t$=1.0s

(d) $t$=1.5s (e) $t$=2.0s (f) $t$=2.5s

(g) $t$=3.0s (h) $t$=3.5s (i) $t$=4.0s

Figure 2: Cylinder velocity with $t$=0.5s time-step

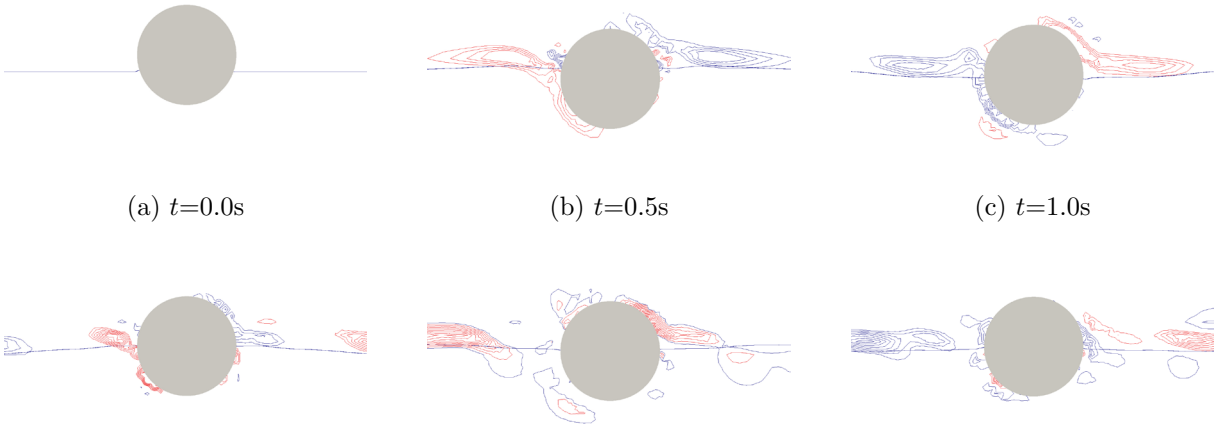

(a) $t$=0.0s (b) $t$=0.5s (c) $t$=1.0s

(d) $t$=1.5s (e) $t$=2.0s (f) $t$=2.5s

Figure 3: Vorticity around the free heaving circular disc

### 4.2 Free Floating Box in Waves

A floating rigid body is simulated in 2D for wave conditions. The degrees of freedom in the simulation are the movement along the X and Z axis and the rotation around Y axis.
The floating body consists of a box or rectangular barge with a length of $l$=0.30m and a height of $h$=0.20m following the experiment realised at Dalian University by Ren et al. [18]. The water depth is $d$=0.4m. The density of the floating body is $\rho$=500kg/m$^3$. The results will be compared with the experiment.
The simulation is performed in a 20m long and 1.5m high tank . The tank is divided in three zones where the initial wave zone is equivalent to one wavelength and the end zone or numerical beach is equal to two wavelengths, for wave generation and absorption, respectively.
For the simulation, the box is positioned at 7m from the start of the tank so the wave reflection does not affect the simulation results. The comparison will be done after some time when the series of waves stabilize and motion starts. For the waves, 2nd-order Stokes theory is used, with a wave period $T$=1.2s, a wave height $H$=0.04m, a wavenumber $k$=3.245m$^{-1}$ and a wavelength of $L$=1.936m. Three different grids are used in the case: 0.025m, 0.01m and 0.005m with a total cells of 800x60, 2000x150 and 4000x300, respectively.
The wave elevation is presented in 4, it shows a good agreement between numerical results and experimental data. The only difference occurs in the trough of the third and fifth wave which is slightly lower than model results.

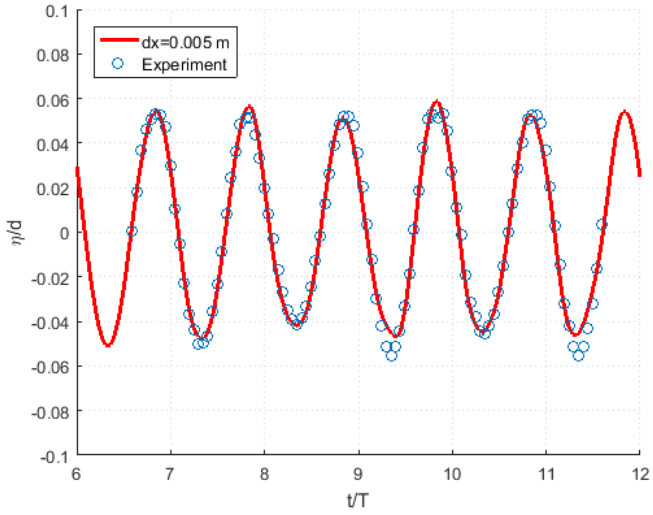


Figure 4: Wave elevation

The numerical heave results in Fig. 5a match the experimental measurements well. The results are accurate in relation to the height except the crests between the first and second waves. All the grids show a good match with the experiment data. In Fig. 5b a detail of the matching part is showed with only the 0.005 grid.

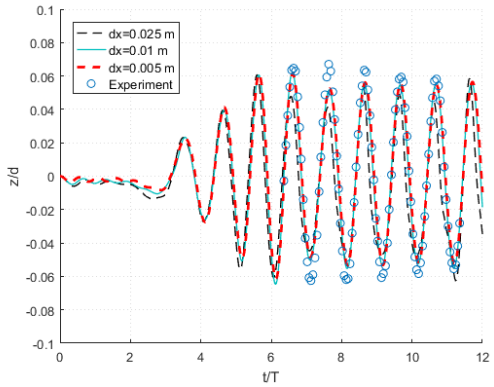


(a) Heave motion with three grid sizes and experiment data

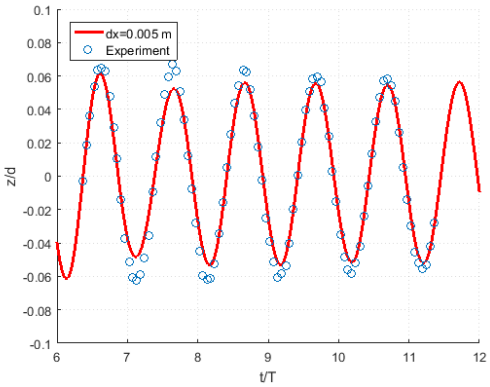


(b) Heave motion between $t/T$=6.0 and $t/T$=12.0

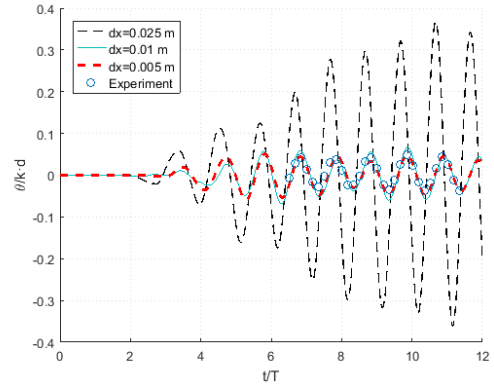


(c) Roll motion with three grid sizes and experiment data

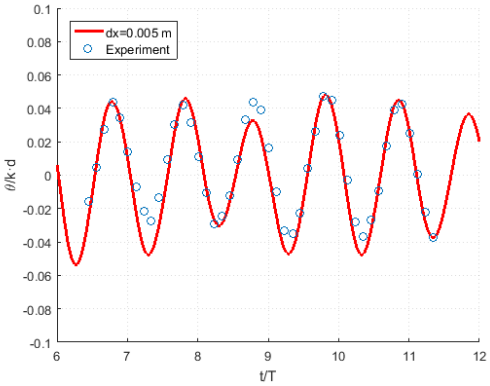


(d) Roll motion between $t/T$=6.0 and $t/T$=12.0

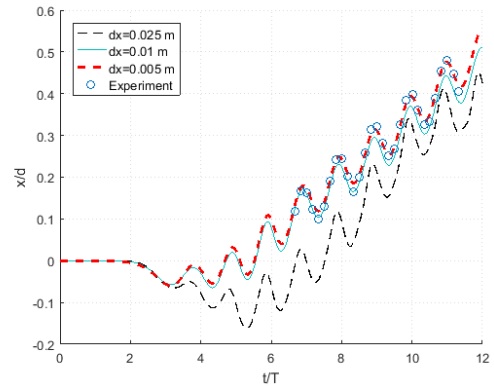


(e) Surge motion with three grid sizes and experiment data

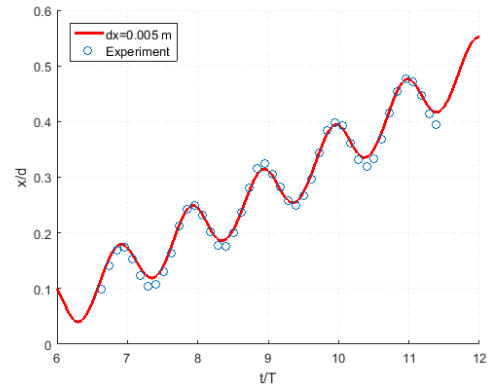


(f) Surge motion between $t/T$=6.0 and $t/T$=12.0

Figure 5: Movement of the free floating box

In Figs. 5c and 5d, the roll motion of the box is presented. The simulated roll peaks almost coincide with the experimental observations. It becomes clear from Fig. 5c, that the coarsest grid with $dx$=0.025m gives unsuitable results, while the two finer meshes perform well. Similar to the other degrees of freedom, the two finer meshes successfully capture the surge motion of the free floating box (Fig. 5e). Fig. 6 shows the contour of the vertical velocity around the floating box at different points in time of the wave.

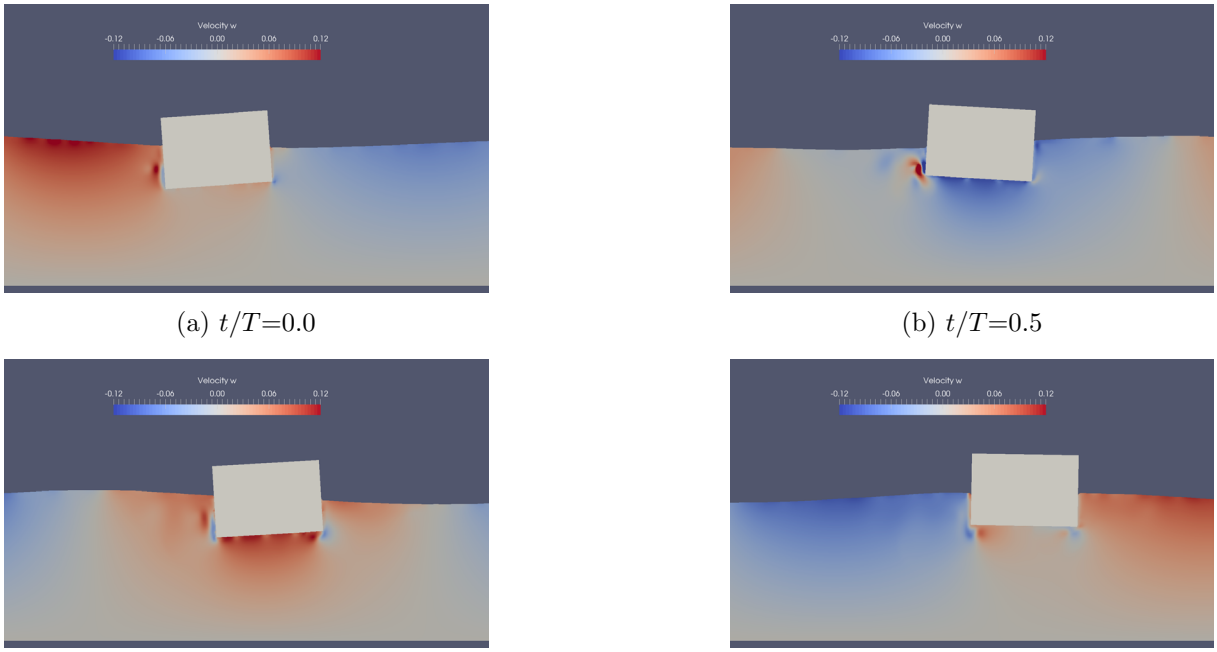


(a) $t/T$=0.0 (b) $t/T$=0.5

(c) $t/T$=1 (d) $t/T$=1.5

Figure 6: Rectangular barge vertical velocity in $t/T$=0.5 intervals

## 5 CONCLUSIONS

The floating body algorithm implemented in REEF3D has been presented, validated and tested for two different cases: a heaving cylinder and a free floating rectangular barge. The cases have been studied with different grid sizes. It has been noted that a grid size of 0.01m presents remarkably good results. For the heaving cylinder, the oscillations in the position of the cylinder match correctly the experimental data. The free floating box matches very well with the experimental data for all the motions. The present study has shown that REEF3D can be used for simulations of floating bodies. However, more studies are needed in relation to floating bodies. The next step would be simulations of floating bodies in a wave field in three dimension to validate all six degrees of freedoms for wave-body interaction. Many structures are moored and the motion of a moored floating body in waves will be targeted in future research.

**ACKNOWLEDGEMENT**

This research was supported in part with computational resources at NTNU provided by The Norwegian Metacenter for Computational Sciences (NOTUR), http://www.notur.no.

**References**

[1] S. F. Ashby and R. D. Flagout. A parallel mulitgrid preconditioned conjugate gradient algorithm for groundwater flow simulations. *Nuclear Science and Engineering*, 124(1):145–159, 1996.

[2] H. Bihs and A. Kamath. Simulation of floating bodies with a combined level set/ghost cell immersed boundary representation. *International Journal for Numerical Methods in Fluids*, 2016.

[3] H. Bihs, A. Kamath, M. Alagan Chella, A. Aggarwal, and Ø. A. Arntsen. A new level set numerical wave tank with improved density interpolation for complex wave hydrodynamics. *Computers & Fluids*, 140:191–208, 2016.

[4] H. Bihs, A. Kamath, M. Alagan Chella, and Ø. A Arntsen. Breaking-wave interaction with tandem cylinders under different impact scenarios. *Journal of Waterway, Port, Coastal, and Ocean Engineering*, 142(5), 2016.

[5] P. M. Carrica, R. V. Wilson, R. W. Noack, and F. Stern. Ship motions using single-phase level set with dynamic overset grids. *Computers and fluids*, 36(9):1415–1433, 2007.

[6] A. Chorin. Numerical solution of the Navier-Stokes equations. *Mathematics of Computation*, 22:745–762, 1968.

[7] R. Croce, M. Griebel, and M. A. Schweitzer. Numerical simulation of bubble and droplet deformation by a level set approach with surface tension in three dimensions. *International journal for numerical methods in fluids*, 62(9):963–993, 2010.

[8] P. A. Durbin. Limiters and wall treatments in applied turbulence modeling. *Fluid Dynamics Research*, 41:1–18, 2009.

[9] R. D. Falgout, J. E. Jones, and U. M. Yang. *Numerical Solution of Partial Differential Equations of Parallel Computers*, chapter The Design and Implementation of hypre, a Library of Parallel High Performance Preconditioners. Lecture Notes in Computational Science and Engineering. Springer, 2006.

[10] Soichi. Ito. Study of the transient heave oscillation of a floating cylinder. BSc thesis, Massachusetts Institue of Technology, Tokyo, Japan, 1971.

[11] G. S. Jiang and D. Peng. Weighted ENO schemes for Hamilton-Jacobi equations. *SIAM Journal on Scientific Computing*, 21:2126–2143, 2000.

[12] G. S. Jiang and C. W. Shu. Efficient implementation of weighted ENO schemes. *Journal of Computational Physics*, 126:202–228, 1996.

[13] A. Kamath, H. Bihs, M. Alagan Chella, and Øivind A Arntsen. Upstream-cylinder and downstream-cylinder influence on the hydrodynamics of a four-cylinder group. *Journal of Waterway, Port, Coastal, and Ocean Engineering*, 2016.

[14] D. Naot and W. Rodi. Calculation of secondary currents in channel flow. *Journal of the Hydraulic Division, ASCE*, 108(8):948–968, 1982.

[15] Muk Chen Ong, Arun Kamath, Hans Bihs, and Mohammad Saud Afzal. Numerical simulation of free-surface waves past two semi-submerged horizontal circular cylinders in tandem. *Marine Structures*, 52:1–14, 2017.

[16] S. Osher and J. A. Sethian. Fronts propagating with curvature- dependent speed: algorithms based on Hamilton-Jacobi formulations. *Journal of Computational Physics*, 79:12–49, 1988.

[17] B. Ramaswamy, M. Kawahara, and T. Nakayama. Lagrangian finite element method for the analysis of two-dimensional sloshing problems. *International Journal for Numerical Methods in Fluids*, 6:659–670, 1986.

[18] B. Ren, M. He, P. Dong, and H. Wen. Nonlinear simulations of wave-induced motions of a freely floating body using WCSPH method. *Applied Ocean Research*, 50:1–12, 2015.

[19] C. W. Shu and S. Osher. Efficient implementation of essentially non-oscillatory shock capturing schemes. *Journal of Computational Physics*, 77:439–471, 1988.

[20] M. Sussman, P. Smereka, and S. Osher. A level set approach for computing solutions to incompressible two-phase flow. *Journal of Computational Physics*, 114:146–159, 1994.

[21] E. Walhorn, A. Kölke, B. Hübner, and D. Dinkler. Fluid–structure coupling within a monolithic model involving free surface flows. *Computer Structures*, 83:2100–2111, 2005.

[22] J. Yang, Z. Wang, and F. Stern. Sharp interface immersed-boundary/level-set method for wave–body interactions. *Journal of Computational Physics*, 228:6590–6616, 2009.